Enhancing the Design of Dynamic Vibration Absorbers through Harmonic Analysis and Lumped Parallel Configuration

Faris A. Jabbar

Department of Mechanical Engineering, Andhra University. Visakhapatnam 530003, India | Technical Institute of Al Dewaniyah, Al-Furat Al-Awsat Technical University (ATU), Al-Dewaniyah, Iraq
farishani349@gmail.com (corresponding author)

Putti Srinivasa Rao

Department of Mechanical Engineering, Andhra University, Visakhapatnam 530003, India
prof.psrinivasarao@andhrauniversity.edu.in

Salwan Obaid Waheed Khafaji

Department of Mechanical Engineering, University of Babylon, Babylon, Iraq
eng.salwon.obaid@uobabylon.edu.iq

ABSTRACT

This work examines the utilization of negative mass and negative stiffness principles to enhance the effectiveness of Dynamic Vibration Absorbers (DVAs) for vibration attenuation developed in structures. The proposed idealized model aims to reduce the amplitude of resonance and expand the frequency stopband range to achieve vibration reduction by attaching two parallel dynamic vibration absorbers to the primary system. By incorporating stiffness, mass, and damping ratio for each one of the absorbers and in the presence of harmonic excitation, it is possible to expand the frequency range in which vibration may be suppressed, leading to a substantial decrease in the maximum vibration amplitude of the primary system and the stroke length of the absorbers. The Nelder-Mead method is successfully used as an optimization tool to obtain the best selection of the absorbers' design parameters that assure the best vibration attenuation and frequency stopband. The results indicate a strong association between the change in frequency and the decrease in vibration. In the instance of frequency response, the vibration amplitude decreased by an average of 91.46% across all three modes of the whole system. Another optimal selection exhibited the most significant enhancement, achieving an average reduction in vibration amplitude of 97.06% across all three modes. Finally, the results indicate that the suggested lumped parallel architecture of the absorbers with precisely adjusted negative mass and negative stiffness characteristics along with the presented optimization method, can greatly improve the effectiveness of reducing vibrations in various applications. The results illustrate a direct relationship between shifts in frequency and vibration. If the value of the shift is greater than 1 the vibration is decreased, while less than 1 means the worst form of reducing such magnitude. The most notable drop off in amplitude occurred when averaging a simple drop off of up to 91.46% for all three patterns where frequency shifts by Y=2.008.

Keywords-dynamic absorber; optimization; stiffness; mass; damping ratio; frequency response; time response

I. INTRODUCTION

Dynamic Vibration Absorbers (DVA) are among the most common vibration control devices because they are effective, long lasting, and inexpensive. Frahm [1] invented the first undamped DVA in 1909, which consisted of a spring and a mass linked to a vibrating body that vibrated harmonically or in a narrowband frequency range. Optimization design studies have shown that vibration absorbers are effective in reducing

vibrations generated by external disturbances and rotational imbalances. Step-response features like peak overrun MP and settling time (t_s) are frequently used as examples. The modified Chebyshev's equioscillation theorem approach is utilized to get the best DVAs for the damping main system. The optimal absorber system for a given primary damping ratio and mass ratio is the combination of attributes that produces the smallest and highest frequency response amplitudes. To address the dampening of the first two flexural modes of a free-free beam,

a 2-DOF TMD is adjusted and shown. Previous studies [2-8] employed the ideal absorber settings to confirm the frequency response's flatness at the first natural frequency, and vibration absorber tuning [9-13] was carried out. Some researchers concentrated on the influence of positive springs, while others developed the idea of negative stiffness, which indicates a reversal in the connection between external force and displacement in deformed structures.

The TMD damping ratio may be optimized to match the maxima of the displacement response transfer function with the "fixed-point" frequencies, resulting in the greatest decrease in structural displacement possible. When a DVA is added to a 1-DoF system, it becomes a new 2-DoF system. Resonance happens when one of the new intrinsic frequencies matches the stimulating frequency. Ant colony optimization has been used to solve the optimization problem. The optimal settings of a non-conventional DVA intended to decrease vibration caused by ground motion in a 1-DoF system were identified. When a 2-DoF absorber has an opposite damper in the primary system, it performs much better than absorbers with solely positive dampers. Authors in [14-20] looked into the characteristics and stability requirements of the negative stiffness system. When compared to a system with solely positive stiffness, a system with Negative Stiffness (NS) has a lower natural frequency and a larger load capacity. Negative stiffness components were used to build compliant composite unit cells, with flexible rubber tubes of silicone in a post-buckled condition providing negative stiffness. The resulting maximum damping is significantly more than the silicone's. Composites (viscoelastic matrix) with negative stiffness, showed higher mechanical damping and stiffness than separate components, exceeding acceptable limits. The dynamics and stability of discrete viscoelastic spring systems with NS components were explored, focusing on extreme aspects. The strength of a discrete viscoelastic system with NS components was investigated in both time and frequency domains. The stability requirements are determined using exact solutions to the DEqns and the Lyapunov stability theorem. The frequency response of the system demonstrates that overall stiffness grows with frequency, reaching infinity when one component has the required NS characteristics.

Hartog [21] advocated using a DVA to increase the frequency range and responsiveness of the primary system. The calculation of optimal DVA parameters was involved, which were then used to compute the frequencies associated with the frequency response. The ideal DVA was defined as limiting the maximum amplitude of the main mass while obtaining equal magnitudes at the two designated sites. This technique became known as the equal-peak method. Previous research [22] concentrated on linear absorbers with undamped primary systems. The authors proved that adding a damper not only increased the frequency range, but also dissipated energy. Authors in [23] presented the use of MDVAs to reduce internal floor low-frequency vibration in a high-speed EMU train. The floor, carbody, and MDVAs make up an improved numerical model that is utilized to calculate transmissibility. The optimum parameters of each DVA were calculated using the transmissibility, and the mode that contributed the most to the response was determined by a contribution analysis. Utilizing

digital simulations and the many scales technique, the vibrations of a non-linear dynamic vibration absorber were examined in [24]. The primary findings relate to certain dynamic instabilities that may arise when the absorber is engineered so that the intended operating frequency roughly corresponds to the average of the two linearized natural frequencies of the system. In [25], the effectiveness of a recently created quadratic vibration absorber that is based on the saturation phenomena was examined both theoretically and empirically. The authors took into account the issue of managing the vibrations of a plant with 1-DoF, developed the equations governing the closed-loop system's responses, and arrived at an approximate solution. To regulate the vibrations of plates, a nonlinear active vibration absorber was studied in [26]. The absorber was based on the two-to-one internal resonance and saturation phenomena found in dynamical systems with quadratic nonlinearities. In the finite-element study, the control was modeled using a user-provided subroutine and the commercial program ABAQUS. Authors in [27] investigated a nonlinear absorber that works well at a variety of forcing amplitudes. A qualitative tuning approach that required the absorber's frequency–energy dependency to match the nonlinear primary system's was developed. Using a nonlinear extension of Hartog's equal-peak approach, the NLTVA parameters were defined. After that, the suggested advancements were examined by looking at how to reduce a Duffing oscillator's resonant vibrations [28]. Warburton [29, 30] examined the ideal damping and tuning ratios for reducing the mean square values of vibration displacement or kinetic energy throughout a frequency range when subjected to diverse external excitations. Authors in [31] investigated a damped single-DoF (SDoF) primary system and obtained analytical solutions for H2 optimization of the absorber parameters as well as series solutions for H- optimization, demonstrating the importance of the Hartog method when the damping of the main system is assumed to be zero. Authors in [32] diverged from optimal absorber settings to investigate the practical response of DVAs. The optimization of DVA settings, taking into account both damped and undamped main systems was approached as an optimization problem, with the objective function constructed using the Hartog method. The goal was to limit the sensitivity of the primary system to harmonic forces or base motion [33]. In [34], the dynamic vibration absorber system was improved by including a Maxwell model with viscoelastic material and varied negative stiffness springs. Using the H1 optimization idea and the fixed-point theory, all system parameters were optimized, including the optimal natural frequency ratio, optimal damping ratio, and the DVA's first optimum negative stiffness ratio. The other ideal negative stiffness ratio was determined by additionally taking system stability into account. In [35], an enhanced beam-based DVA was presented for minimizing resonant vibration in general structures, with vibration suppression efficacy determined by the length of the beam, flexural stiffness, and mass ratio. An extended optimality criteria technique was deployed to generate simultaneous equations for this design issue, guaranteeing that the amplitudes of the two peaks in the resonance curve were properly tuned, resulting in minimal amplitude amplification. These simultaneous equations were solved using ordinary numerical computing applications. The

performance development of the DVA over the traditional Voigt type was evaluated using comparable mass ratios [36].

To improve the low-frequency control capabilities of a grounded DVA, an amplification mechanism and grounded stiffness element were introduced in [37]. The ideal grounded stiffness ratio may be negative, zero, or positive, depending on the mass and magnification ratios. H2 optimization was utilized to calculate the variance of the squared modulus of the undamped frequency response of the main structure. Non-linear unconstrained optimization problems were developed to find the optimal design in [38]. To decrease vibration responses in actual applications, particular platforms were proposed with a Vibration Isolation and Mitigation (VIM) system that includes Magnetrheological (MR) and viscoelastic (VE) dampers. In [39], the Non-dominated Sorting Genetic Algorithm (NSGA-II) was employed in the optimization strategy, with maximum damping forces of the MR dampers chosen as objective functions.

The perfectly constructed Multiple-Tuned Mass Damper Inerter (M-TMDI) [40] outperformed the TMD and the three-element TMD in terms of static stretching, stroke limitation, and steady-state amplitude. The effective mass ratio, which is determined by the inserter position, mode shape, physical mass and inertial mass, was critical in obtaining the maximum control of the M-TMDI. In [41], a grounded-type DVA with a lever component was proposed to increase control performance by increasing effective mass and decreasing inefficient mass. To improve ride comfort in active suspension systems, a finite-frequency H∞ controller was created by linear matrix inequality optimization in [42]. The operating area and capacity of the suspensions system to maintain road contact, were evaluated throughout both phases of the controller design. The study used the two-fixed point approach and H∞ maximization criterion to optimize the components of a DVA. The optimal values of the grounded stiffness and tuned mass damper components, were calculated to lower resonant amplitude in an undamped system under harmonic excitation [34]. To decrease low-frequency vibration in joist floor structures, an optimization strategy for several DVA design parameters was developed. An analytical model that included the motion of a plate and beams was utilized to calculate the vibration of the joist floor construction [43, 44]. The absorber and energy harvester properties were optimized using genetic algorithms and response surface approaches. Both linear and nonlinear primary systems were studied, and validation was performed using analytical solutions from the literature [45].

Passive DVAs are widely employed to minimize structural vibration, but there is a need for more efficient ones. Authors in [46] proposed novel inserter-based DVAs to improve the performance of passive DVAs. Four kinds of inserter-based DVAs with negative stiffness (IN-DVAs) were introduced and fully tested. The fixed-point theory [47] was adopted to establish the optimal settings for each kind of IN-DVA. Overall, the investigations addressed many elements of dynamic vibration absorbers, such as design, optimization, and performance enhancement strategies. These discoveries improved the effectiveness of vibration control systems in a wide range of applications. Base isolation of huge equipment involves various challenges. Due to their large size, these machines rely on structures with static stiffness for support. Furthermore, they frequently operate at low frequencies. When in operation, these devices operate like simple mass-spring oscillators. Vibrations from the machine support, which acts as an elastic spring, might travel to the surrounding building or the ground, causing unwanted noise and vibration transmission. Several techniques have been investigated to reduce vibration transmission through the supports [48]. One solution, presented in [49], employed buckling beams under axial stress to generate NS around the equilibrium position. The NS was then paired with a linear positive spring to create an isolation mechanism. Authors in [50, 51] used an active control strategy to achieve NS and presented a unique vibration isolation technology. Furthermore, authors in [52] conducted analytical and experimental studies on a passive DVA that uses an NS mechanism. Similarly, authors in [53–55] investigated nonlinear vibration isolators employing negative stiffness methods. However, the current analytical methods for optimal parameters are time-consuming, limited in scope, and may not be useful when design parameters change [56]. A finite element approach for twin beams under static stress was developed in [57]. The displacements of the upper and lower beams were determined by an MATLAB algorithm. The excellent accuracy of the proposed technique was illustrated by comparing the numerical examples with the analytical solution.

Based on the information gained from previous works, it can be concluded that several problems were addressed and need to be investigated for the useful application of dynamic vibration absorber, such as detailed mathematical modeling that makes it more understandable and the use of inefficient optimization algorithms, which are time-consuming, limited in scope, and may not be useful when design parameters change. The authors developed a mathematical modeling of two parallel DVAs that allows for trade-offs between all of these constraints. To aid in the design of a dynamic absorber with improved performance, the concepts of negative stiffness, mass, and damping ratio were carefully introduced and investigated, as well as their physical explanations. The concept of a 2-DoF vibration absorber was extended to create a broadband vibration absorber capable of dispersing vibrational energy across a wide frequency range. Initially, a 3-DoF system was used to demonstrate this idea. Harmonic analysis was then applied to evaluate the harmonic response to external stimulation to fulfill optimization objectives and acquire the best design parameters. As far as is known, this is the first trial of finding the relationship between frequency shift and vibration reduction in the main system based on a simple and efficient equation.

II. MATHEMATICAL MODELING

A. Design of a Spring-Mass Absorber for Vibration Attenuation

The 3-DoF system is presented in Figure 1.
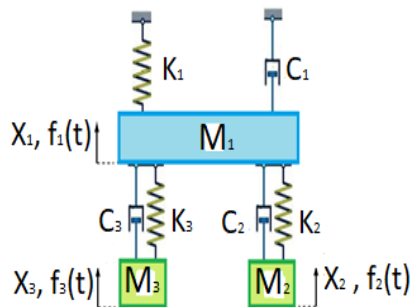
Fig. 1.   The damping 3 DoF vibratory system.

The corresponding displacements are denoted as X_1, X_2, and X_3 for masses M_1, M_2, and M_3. The multi-frequency vibration absorber works by enforcing the locally resonant frequencies, ω_i, equal to the excitation frequency ω, resulting in X_1 equal to zero. Figure 1 shows the main construction with two lumped masses functioning as vibration absorbers. Two parallel masses, M_2 and M_3, and springs with constants K_2 and K_3 are coupled to the basic structure of mass M_1. The spring with constant K_1 is also coupled to the main structure. The governing differential equations are derived as follows:

$$\begin{bmatrix} M_1 & 0 & 0 \\ 0 & M_2 & 0 \\ 0 & 0 & M_3 \end{bmatrix} \begin{Bmatrix} X_1'' \\ X_2'' \\ X_3'' \end{Bmatrix} +$$

$$\begin{bmatrix} C_1+C_2+C_3 & -C_2 & -C_3 \\ -C_2 & C_2 & 0 \\ -C_3 & 0 & C_3 \end{bmatrix} \begin{Bmatrix} X_1' \\ X_2' \\ X_3' \end{Bmatrix} +$$

$$\begin{bmatrix} k_1+k_2+k_3 & -k_2 & -k_3 \\ -k_2 & k_2 & 0 \\ -k_3 & 0 & k_3 \end{bmatrix} \begin{Bmatrix} X_1 \\ X_2 \\ X_3 \end{Bmatrix}$$

$$= \begin{Bmatrix} f_1(t) \\ f_2(t) \\ f_3(t) \end{Bmatrix} \tag{1}$$

where $f_1(t)$, $f_2(t)$, and $f_3(t)$ are the loads applied. The force vector is:

$$\begin{aligned} f_1(t) &= F_1 e^{jwt} \\ f_2(t) &= F_2 e^{jwt} \\ f_3(t) &= F_3 e^{jwt} \end{aligned} \tag{2}$$

where w is the excitation frequency. The general solution of (1) can be presumed as:

$$x_i = X_i(j\omega)e^{jwt} \tag{3}$$

$$a_{ip} = -M_{ip}\omega^2 + jC_{ip} + K_{ip} \tag{4}$$

where i_p = 1, 2, 3. The index i refers to the first, second, and third coordinates of the system, respectively. Using (1), (2), and (3), the mathematical modeling can be given by:

$$\begin{bmatrix} a_{11}(j\omega) & a_{12}(j\omega) & a_{13}(j\omega) \\ a_{21}(j\omega) & a_{22}(j\omega) & a_{23}(j\omega) \\ a_{31}(j\omega) & a_{32}(j\omega) & a_{33}(j\omega) \end{bmatrix} \begin{Bmatrix} X_1(j\omega) \\ X_2(j\omega) \\ X_3(j\omega) \end{Bmatrix} = \begin{bmatrix} F_1 \\ F_2 \\ F_3 \end{bmatrix} \tag{5}$$

Equation (5) is solved for obtaining the amplitude of the presumed time response as follows:

$$\begin{aligned} X_1(j\omega) &= F_1 \begin{bmatrix} a_{22}(j\omega)a_{33}(j\omega) - a_{23}(j\omega) \\ a_{32}(j\omega) \end{bmatrix} \\ &- F_2[a_{12}(j\omega)a_{33}(j\omega) - a_{13}(j\omega)a_{32}(j\omega)] \\ &+ F_3[a_{12}(j\omega)a_{23}(j\omega) - a_{13}(j\omega)a_{22}(j\omega)] \\ &/ D_o(j\omega) \end{aligned}$$

$$\begin{aligned} X_2(j\omega) &= F_1 \begin{bmatrix} a_{21}(j\omega)a_{33}(j\omega) - a_{23}(j\omega) \\ a_{31}(j\omega) \end{bmatrix} \\ &- F_2[a_{11}(j\omega)a_{33}(j\omega) - a_{13}(j\omega)a_{31}(j\omega)] \\ &+ F_3[a_{11}(j\omega)a_{23}(j\omega) - a_{13}(j\omega)a_{21}(j\omega)] \\ &/ D_o(j\omega) \end{aligned} \tag{6}$$

$$\begin{aligned} X_3(j\omega) &= F_1 \begin{bmatrix} a_{21}(j\omega)a_{32}(j\omega) - a_{22}(j\omega) \\ a_{31}(j\omega) \end{bmatrix} \\ &- F_2[a_{11}(j\omega)a_{32}(j\omega) - a_{12}(j\omega)a_{31}(j\omega)] \\ &+ F_3[a_{11}(j\omega)a_{22}(j\omega) - a_{12}(j\omega)a_{21}(j\omega)] \\ &/ D_o(j\omega) \end{aligned}$$

$$\begin{aligned} D_o(j\omega) &= \begin{bmatrix} a_{11}(j\omega)a_{22}(j\omega)a_{33}(j\omega) - a_{11}(j\omega) \\ a_{23}(j\omega)a_{32}(j\omega) \end{bmatrix} \\ &- \begin{bmatrix} a_{12}(j\omega)a_{21}(j\omega)a_{33}(j\omega) - a_{12}(j\omega)a_{23}(j\omega) \\ a_{31}(j\omega) \end{bmatrix} \\ &+ \begin{bmatrix} a_{13}(j\omega)a_{21}(j\omega)a_{32}(j\omega) - a_{13}(j\omega)a_{22}(j\omega) \\ a_{31}(j\omega) \end{bmatrix} \end{aligned} \tag{7}$$

To study the vibration effect, the forces $F2$ and $F3$ are set to zero and (6) can be updated as:

$$\beta G_{11}(j\omega) = \frac{\beta X_1(j\omega)}{F_1} = \beta \frac{\begin{bmatrix} a_{22}(j\omega)a_{33}(j\omega) - \\ a_{23}(j\omega)a_{32}(j\omega) \end{bmatrix}}{D_o(j\omega)}$$

$$\beta G_{21}(j\omega) = \frac{\beta X_2(j\omega)}{F_1} = -\beta \frac{\begin{bmatrix} a_{21}(j\omega)a_{33}(j\omega) \\ - a_{23}(j\omega)a_{31}(j\omega) \end{bmatrix}}{D_o(j\omega)} \tag{8}$$

$$\beta G_{31}(j\omega) = \frac{\beta X_3(j\omega)}{F_1} = \beta \frac{\begin{bmatrix} a_{21}(j\omega)a_{32}(j\omega) - \\ a_{22}(j\omega)a_{31}(j\omega) \end{bmatrix}}{D_o(j\omega)}$$

where $\beta G_{11}(j\omega)$, $\beta G_{21}(j\omega)$, and $\beta G_{31}(j\omega)$ are frequency-response functions due to F_1 only. The parameter β (N/m) is a parameter introduced to make (9) non-dimensional. The general form of the frequency response can be given by:

$$H_{ij} = \beta \, | G_{ij}(j\omega) |, \;\; ij = 1,2,3 \qquad (9)$$

Back to the system presented in Figure 1, the matrix $a_{ij}(j\omega)$ given in (5), with some non-dimensional parameters, can be determined by:

$$a_{11}(j\omega) = k_1 A(j\Omega)$$
$$a_{12}(j\omega) = -k_1 m_r B(j\Omega)$$
$$a_{13}(j\omega) = -k_1 \frac{m_3}{m_1} C(j\Omega)$$
$$a_{21}(j\omega) = -k_1 m_r B(j\Omega)$$
$$a_{22}(j\omega) = k_1 m_r D(j\Omega) \qquad (10)$$
$$a_{23}(j\omega) = 0$$
$$a_{31}(j\omega) = -k_1 \frac{m_3}{m_1} C(j\Omega)$$
$$a_{32}(j\omega) = 0$$
$$a_{33}(j\omega) = k_1 \frac{m_3}{m_1} E(j\Omega)$$

$$\Omega = \frac{\omega}{\omega_{n1}}; \; \omega_r = \frac{\omega_{n2}}{\omega_{n1}}; 2\xi = \frac{C_i}{m_i \omega_{ni}} \qquad (11)$$

$$A(j\Omega) = -\Omega^2 + 2j\Omega\left(\xi_1 + \xi_2 m_r \omega_r + \xi_3 \frac{m_3}{m_1}\frac{\omega_{n3}}{\omega_{n1}}\right)$$
$$+ 1 + m_r \omega_r^2 + \frac{m_3}{m_1}\frac{\omega_{n3}^2}{\omega_{n1}^2}$$

$$B(j\Omega) = 2j\Omega\xi_2 \omega_r + \omega_r^2$$

$$C(j\Omega) = 2j\Omega\xi_2 \frac{\omega_{n3}}{\omega_{n1}} + \frac{\omega_{n3}^2}{\omega_{n1}^2} \qquad (12)$$

$$D(j\Omega) = -\Omega^2 + 2j\Omega\xi_2 \omega_r + \omega_r^2$$

$$E(j\Omega) = -\Omega^2 + 2j\Omega\xi_2 \frac{\omega_{n3}}{\omega_{n1}} + \frac{\omega_{n3}^2}{\omega_{n1}^2}$$

Finally, the frequency response functions, described by (9), can be given as:

$$H_{11}(j\omega) = k_1 |G_{11}(j\omega)| =$$
$$\left[\begin{array}{c} \left\{-\Omega^2 + 2j\Omega\xi_2\omega_r + \omega_r^2\right\} \\ \left\{-\Omega^2 + 2j\Omega\xi_2 \frac{\omega_{n3}}{\omega_{n1}} + \frac{\omega_{n3}^2}{\omega_{n1}^2}\right\} \end{array}\right] / D_o(j\Omega)$$
$$\qquad (13)$$

$$H_{21}(j\omega) = k_1 |G_{21}(j\omega)| =$$
$$\left[\begin{array}{c} \left\{2j\Omega\xi_2\omega_r + \omega_r^2\right\} \\ \left\{-\Omega^2 + 2j\Omega\xi_2 \frac{\omega_{n3}}{\omega_{n1}} + \frac{\omega_{n3}^2}{\omega_{n1}^2}\right\} \end{array}\right] / D_o(j\Omega)$$

$$H_{31}(j\omega) = k_1 |G_{31}(j\omega)| =$$
$$\left[\begin{array}{c} \left\{-\Omega^2 + 2j\Omega\xi_2\omega_r + \omega_r^2\right\} \\ \left\{2j\Omega\xi_2 \frac{\omega_{n3}}{\omega_{n1}} + \frac{\omega_{n3}^2}{\omega_{n1}^2}\right\} \end{array}\right] / D_o(j\Omega)$$

B. Optimization

1) Probabilistic Restart

When local optimizers are initiated from different points repeatedly, they can be combined to form a global search. The most basic restart techniques initiate the search either from a randomly selected point set or from a regular grid of points. In the first scenario, the number of restarts necessary to determine the mesh size, must be known. In the other scenario, previous search history is not utilized, which increases the likelihood of finding the same local optima repeatedly and incurs significant needless effort. The Gaussian Parzen-Windows method characterizes the sampling probability of a point x, $p(x)$ [58]. This approach is a smoother variation of the histogram procedures because the histograms are centered at specific sampling points. The expression for the probability $p(x)$ is:

$$P(x) = \frac{1}{N} \sum_{i=1}^{N} P_i(x) \qquad (14)$$

where P_i is the density function of the normal multidimensional probability and N is the number of sampled points. For more convents, (14) can be expanded as:

$$P_i(x) = \frac{1}{(2\pi)^{\frac{n}{2}}(\det(\Sigma))^{\frac{1}{2}}} \times$$
$$\exp\left(-\frac{1}{2}(x - x_i)^T \Sigma^{-1}(x - x_i)\right) \qquad (15)$$

where n is the number of variables and Σ represents the covariance matrix:

$$\Sigma = \begin{bmatrix} \sigma_1^2 & 0 \\ 0 & \sigma_n^2 \end{bmatrix} \qquad (16)$$

$$\sigma_k^2 = \alpha\left(x_k^{\max} - x_k^{\min}\right)^2 \qquad (17)$$

The parameter α regulates the Gaussians length and $x_k^{\max}$ and $x_k^{\min}$ are the bonds of the jth direction. The variances are maintained constant to keep the procedure as straightforward and affordable as possible. The overall number of analyses required for this method would be expensive. The probability density is such that:

$$\int_{-\infty}^{\infty} P(x)dx = 1$$

The bounded probability can be described as:

$$\tilde{P}(x) = \frac{P(x)}{M}; \; M = \int_{\Omega} P(x)dx \qquad (18)$$

The likelihood of not having previously sampled x is represented by the sampling probability density as $\phi(x)$:

$$\phi(x) = \frac{H - \tilde{P}(x)}{\int_{\Omega}\left(H - \tilde{P}(x)\right)dx};$$

(19)

such that $H = \max \tilde{P}(x)$.

The maximization is not carried out exactly for two reasons: (1) due to its numerical cost and (2) because it would negatively affect the search. Instead, a random selection of points is made, and the point that maximizes ϕ is chosen to start the next round. In the other hand, maximizing ϕ requires calculating only p because the maximum value of ϕ is the minimum of p. Due to these limitations, a modified Nelder-Mead Method is used in this work to get better results.

2) The Nelder-Mead Method

A numerical approach for figuring out an objective minimum or maximum function in a multidimensional space is the Nelder-Mead method. It is also referred to as the polytope technique, the Amoeba method, and the downhill simplex approach. This method of direct search is applied to non-linear problems. This methodology is a heuristic search strategy that, when used to solve problems that can be solved in different ways, can converge to non-stationary points [59, 60]. The criteria utilized to estimate the convergence of the method are the degenerate simplex and flat tests. The simplex is the smaller if (20) is satisfied [61, 62]:

$$k = \min_{1...n+1}\left(\sum_{k=1}^{n}\left|\frac{x_i^k}{x_i^{\max} - x_i^{\min}}\right|\right)\langle \varepsilon_{s1}$$

(20)

where $x_i^{\max}$ and $x_i^{\min}$ are the bounds in the ith direction, and ε_{s1} is the termination tolerance.

III. RESULTS AND DISCUSSION

The objective of this work is to investigate the effect of the more sensitive parameters of a spring-mass absorber and obtain the optimal values of a unit cell absorber (optimal spring, optimal mass, and optimal damping ratio for the absorber) to enhance absorption capacity and vibration attenuation. Furthermore, two DVAs in parallel are used instead of one for controlling the dynamic response of the structures.

A. Paremetric Study

1) Frequency Response

Several cases are considered to clarify the influence of the design parameters of the DVA on the frequency range. In general, the frequency response indicates how a certain attribute changes the response to an input as a function of the excitation frequency. A frequency sweep, or solving for several distinct frequencies, is required to generate a frequency response curve. The frequency response curve shows several discrete peaks at the system frequencies.

a) Case 1: Frequency Response without and with DVA

Figure 2(a) presents the frequency response function of the base plate (H_{11}). The peak will occur when the excitation frequency reaches 10 Hz when no DVA is attached. Two peaks

are developed on each side of the initial peak. The stop bands for the 3-DoF system are noticed between the two frequency values that lie between three peaks. There must be two stop bands around each local frequency to absorb multi-frequency vibrations with two lumped masses and, therefore, two resonant frequencies [63-66]. The two local resonant frequencies are close to each other, so selecting the appropriate damping results in a broader stop band range, as evidenced in Figure 2(b). The two absorbers behave as a single absorber (same magnitudes of mass, springs, and dampers) resulting in just two natural frequencies at peak positions. This causes the response to be similar to that of a 2-DoF vibration control system [67], as observed in Table I.

(a)

(b)
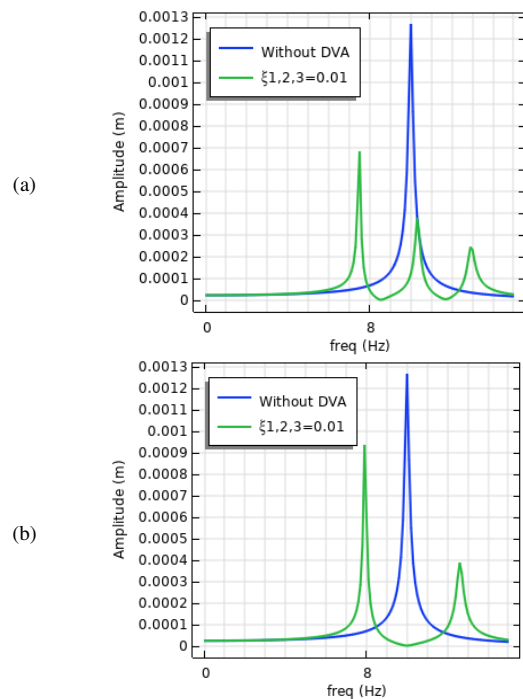
Fig. 2.   Case 1: Frequency Response of (a) M_1=10 g with $M_2 = M_3 = 0$, $\xi_1 = 0.01$, $\xi_2 = \xi_3 = 0$ (blue), $\xi_1 = \xi_2 = \xi_3 = 0.01$ (green) [66], (b) $\xi_1 = 0.01$, $\xi_2 = \xi_3 = 0$ (blue), $\xi_1 = \xi_2 = \xi_3 = 0.01$ (green) (current work).

TABLE I.   NATURAL FREQUENCY OF THE CURRENT WORK AND [66]

Eigenfrequency (Hz) [66]	Eigenfrequency (Hz) - current work
7.4794	7.9216
10.323	9.9900
12.922	12.608

b) Case 2: Influence of the Damping Factors on the Frequency Response

The amplitude of the base mass is presented in Figure 3. It is commonly known that a small damping system responds quickly to a transient stimulation but that, once the excitation stops, the system gradually reduces its vibration. In Figures 4 and 5, the larger ξ_3 and ξ_2 decreased the amplitude of vibration (red). To fully investigate the influence of ξ_2 and ξ_3, different ξ_3 along with $M_1 = 10$ g and $M_2 = 2$ g, $\xi_1 = \xi_2 = \xi_3 = 0.01$ and different ξ_2 along with $M_1 = 10$ g, $M_2 = 2$ g and $\xi_1 = \xi_2 = \xi_3 = $

0.01 were chosen separately. Larger ξ_3 and ξ_2 significantly reduced the base amplitude at all resonance frequencies.
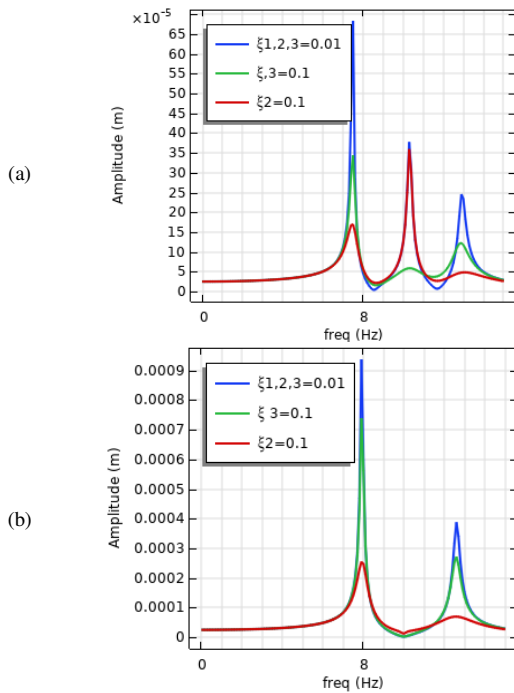
Fig. 3.   Case 2: Frequency response of M_1 = 10 g with M_2 = 2 g and $\xi_1 =\xi_2 = \xi_3$= 0.01 (blue), $\xi_1 =\xi_2$ =0.01, ξ_3 = 0.1 (green), $\xi_1 =\xi_3$ = 0.01, ξ_2 = 0.1 (red). (a) [66], (b) current study.
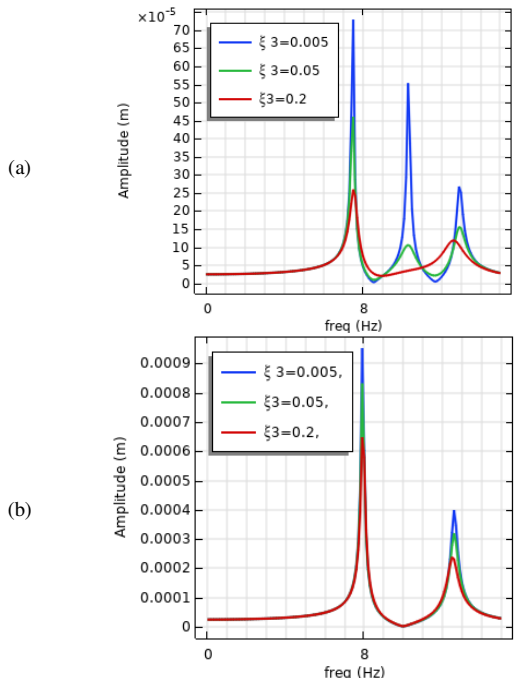
Fig. 4.   Case 2 Frequency response of M_1 = 10 g with M_2 = 2 g, $\xi_1 =\xi_2 =$ 0.01, and ξ_3= 0.005 (blue), ξ_3 = 0.05 (green), ξ_3 = 0.2 (red), (a) [66], (b) current study.
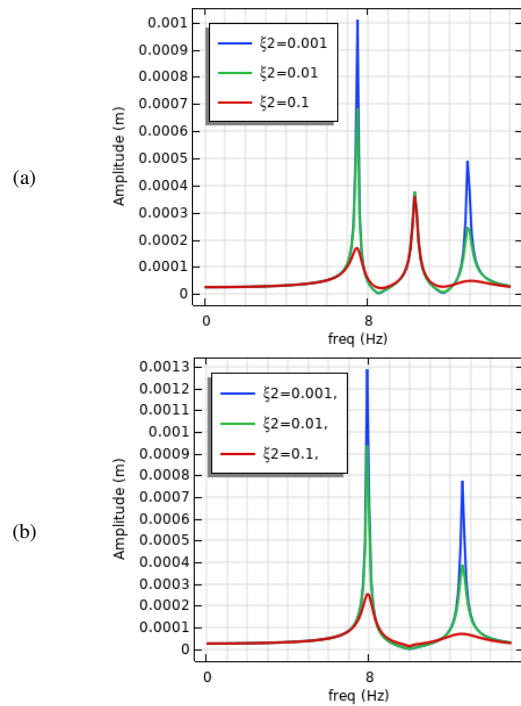
Fig. 5.   Case 2: Frequency response of M_1 = 10 g with M_2 = 2 g, $\xi_1 =\xi_3 =$ 0.01, ξ_2= 0.001 (blue), ξ_2 = 0.01 (green), ξ_2 = 0.1 (red). (a) [66], (b) current study.

c) Case 3: The Effects of M_2, M_3, K_2, and K_3 to the Frequency Response

The FRFs corresponding to M_1, M_2, and M_3 are presented in Figure 6. The two absorbers act as a single absorber since they have the same mass, spring, and damper, resulting in just two natural frequencies at the peak positions. As a result, the response is equivalent to that of a 2-DoF system. When the shifting frequency of the DVA decreases, a bigger M_2 can significantly reduce the amplitude of M_1. In contrast, a small value of M_2 increases the amplitude of vibration with increased shifting frequency. It seems that a small value of M_3 has a minimum impact on the vibration amplitude. The effects of stiffness are displayed in Figure 6(c-d). Bigger K_2 significantly reduced the amplitude of M_1. In contrast, a small value of K_2 increased the amplitude of vibration with increased shifting frequency, while a small value of K_3 showed a minimum effect on the vibration amplitude.

The findings revealed that the addition of DVAs for various values of stiffness and mass affected the produced system frequency and the amplitude change percentage. A machine's ability to operate within a specific frequency range might make the frequency shift effect significant. A DVA installation that causes the system frequency to exceed the permitted range may have an impact on the machinery's effectiveness and efficiency. In some circumstances, sensors can also be used to track the vibration levels of a machine or a building. Included DVAs may alter the system frequency, making it impossible for the sensors to measure the vibration's intensity precisely. This could lead to inaccurate knowledge and, eventually, bad decision-making. So, it is essential to strike a balance between

lowering the vibration amplitude and minimizing any frequency shifts in the system while designing a DVA. In other cases, the main objective can be to reduce the vibration amplitude. In these cases, a DVA-induced frequency shift might even be advantageous [68]. Because of this, the unique design and operational environment of the system must be carefully taken into account while creating and implementing a DVA.

(a)

(b)

(c)

(d)

Fig. 6.   Case 3: The effect of M_2, M_3, K_2, and K_3 to the frequency response.

To obtain the necessary level of vibration reduction and minimize any unwanted consequences, the design must also be improved. As portrayed in Table II, the relationship involves the amplitude percentage change (X), which represents the ratio of the amplitude of the main mass with and without DVA, respectively, such that:

$$X = \frac{aver.ampl.}{without\ DVA} - 1$$

The matching percentage shifting frequency for each of the three modes for every case discussed in this study (Y), which represents relationship between the percentage shifting frequency (APC) to the overall shifting, is defined by:

$$Y = \frac{APC\%}{\sum shifting} - 1$$

When the value (Y) is greater than 1, it indicates a decrease in vibration and when it is less than 1, it indicates a reduction of vibration, which is the worst case. The frequency response results Case 2 (red) showed an average reduction of 91.46% and Y= 2.008 for all three modes. On the other hand, it is noticed for Case 3 that the average decrease for X is 97.06% and Y= 6.19 for all three modes, (the optimal Case 3 is depicted in red). The Case 2 (blue) with X=45.60% and Y = 0.5 was the worst.

B. Optimization Study

Optimization methods can be followed to find the best feasible solution to a well-defined problem. Optimization methods are extensively employed across various fields to identify solutions that either maximize or minimize specific research attributes. These attributes can include minimizing costs in the production of goods or services, optimizing profits, reducing raw material requirements in the manufacturing process of a product, or maximizing output.

1) Case 1: The Influence of M_2 and M_3 Optimization

Figure 7 illustrates the base mass with various M_2 and M_3 values. In Figure 7(c), although M_2 at its optimal value (M_2=0.068, green curve) increases the amplitude of vibration in the first peak, the stop bands are broader and the frequency responses of the second peak are reduced by employing larger M_2 and M_3.

2) Case 1: The Influence of K_2 and K_3 Optimization

Figure 8 shows the effect of the smaller and larger values of stiffness K_2 on the amplitude response. The optimal value of K_2 is 7.987 N/m. Higher stiffness (K_2 and K_3) widen stop bands and boost second peak frequency responses.

3) Case 1: The Influence of ξ_2 and ξ_3 Optimization

Figure 9(a,b) demonstrates how significantly bigger ξ_2 and ξ_3 could decrease the base amplitude at each resonant frequency (red). In contrast, a small value of ξ_2 and ξ_3 (blue) increases the amplitude of vibration. In the first mode, an increase in ξ_2 results in a decrease in vibration amplitude, whereas an increase in ξ_3 causes an increase.

(a)

(b)

(c)
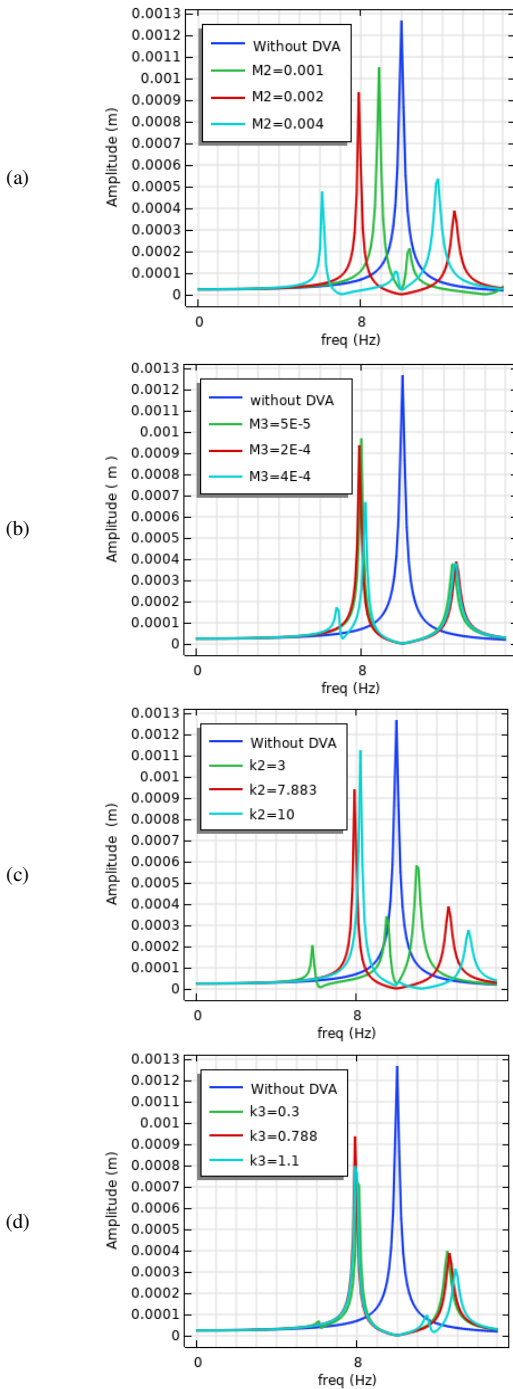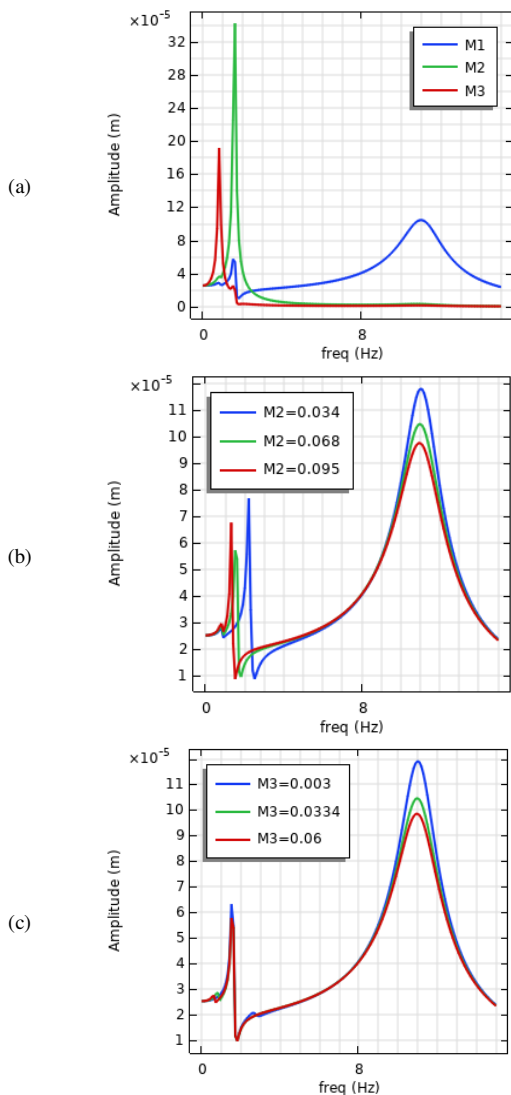
Fig. 7.   Case 1: Optimization for (a) all M_1 = 0.01 kg, M_2 = 0.068 kg, M_3 = 0.0334 kg, K_1 = 39.538 N/m, K_2 = 7.987 N/m, K_3 = 0.888 N/m, ξ_1 = 0.04, ξ_2 = 0.04, ξ_3 = 0.073333, (b) M_2 = 0.034, 0.068, 0.095 (optimal value, green curve), (c) M_3 = 0.003, 0.033, 0.060 (optimal value, green curve).

(a)

(b)
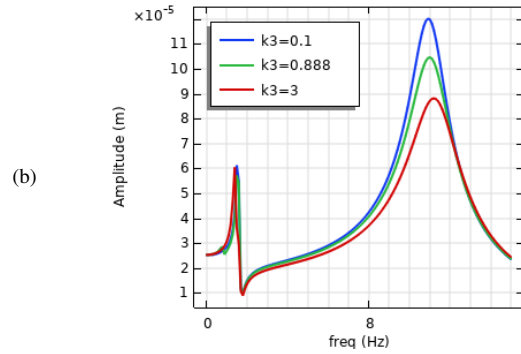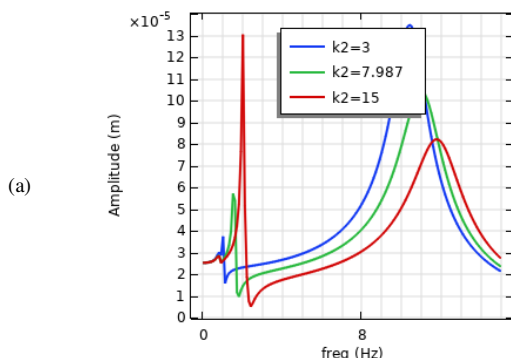
Fig. 8.   Case 2: Optimization for All-(green) M_1 = 0.01 kg, M_2 = 0.068 kg, M_3 = 0.0334 kg, K_1 = 39.538 N/m, K_2 = 7.987 N/m (optimal), K_3 = 0.888 N/m (optimal), ξ_1 = 0.04, ξ_2 = 0.04, ξ_3 = 0.073333, (a) K_2 = 3, 7.987, 15, (b) K_3 = 0.1, 0.888, 3.

The excitation force will be resisted by the damping force that ξ_2 introduces. The transition time to the steady state increases as ξ_2 grows larger. A lower value for ξ_2 is preferred to provide a rapid response to a brief stimulation. Consequently, by employing larger values of ξ_2 and ξ_3, a rapid dissipation in the transient vibration is noticed by activating the vibration absorber directly, which decreases the amplitude of the base mass, and combines two stop bands into a larger stop band.

(a)

(b)
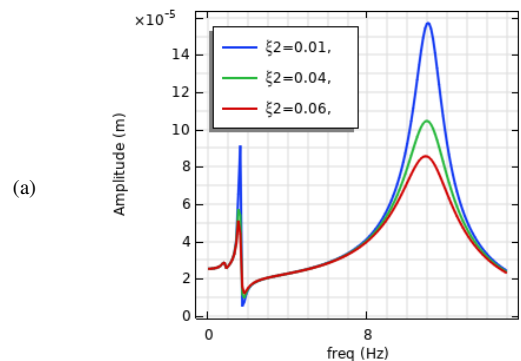
Fig. 9.   Case 3: Optimization for All-(green) M_1 = 0.01 kg, M_2 = 0.068 kg, M_3 = 0.0334 kg, K_1 = 39.538 N/m, K_2 = 7.987 N/m, K_3 = 0.888 N/m, ξ_1 = 0.04, ξ_2 = 0.04, ξ_3 = 0.073333, (a) ξ_2 = 0.01, 0.04, 0.06, (b) ξ_3 = 0.03, 0.0733, 1.1

4) Response Time due to Resonance

The response time of a system is a useful measure of its dynamic features, including variations in its potential, kinetic, and dissipation energy during the response period. It provides

an insightful indicator of how these energies grow and transform throughout the system activity. The resonance response begins small and steadily increases in systems near their inherent frequencies. This phenomenon results from the interaction of the driving force (input) with the system's inherent frequencies. To get a better illustration of the effect of adding a dynamic vibration absorber to the main system, in this work, the system is motivated by an external force that causes a resonance response without adding a dynamic vibration absorber, where the maximum displacement is 0.00125 m, as shown in Table II. The amplitude of the system response is greatly increased. However, due to energy transmission and internal dynamics, the system needs time to build up and

achieve its maximal reaction during the early phase. The driving force transfers energy to the system. However, the system may not be able to instantaneously absorb and distribute this energy efficiently. As a result, the response starts small and gradually accumulates as more energy is transferred and stored within the system. In addition, the presence of damping in the system causes the amplitude of the response to increase gradually. Damping dissipates energy, slowing down the growth rate of the response. This behavior is clearly presented in Figure 10, where the addition of the dynamic vibration absorber has affected the time response due to resonance by enhancing passive damping.

TABLE II.   RELATIONSHIP BETWEEN THE REDUCTION OF VIBRATION AND SHIFTING FREQUENCY

No.		Cases	1st mode	2nd mode	3rd mode	$X=\frac{aver.ampl.}{without\,DVA}-1$ without = 0.00125	APC %	$\sum shifting$	$Y=\frac{APC\%}{\sum shifting}-1$
1		Blue	0.00068	0.00038	0.00025	- 0.6506	65.06	30.71	1.11
2	Case-2 (a) [66]	Green	0.00034	0.00005	0.00013	- 0.8613	86.13	30.71	1.80
3		Red	0.00017	0.00037	0.00013	- 0.8213	82.13	30.71	1.67
4		Blue	0.00093	0	0.00038	- 0.6506	65.06	30.4	1.14
5	Case 2 (a) current work	Green	0.00074	0	0.00025	- 0.736	73.60	30.4	1.42
6		Red	0.00025	0.00002	0.00005	- 0.9146	91.46	30.4	2.008
7		Blue	0.00073	0.00055	0.00027	- 0.5866	58.66	30.71	0.908
8	Case 2 (b) [66]	Green	0.00045	0.00010	0.00015	- 0.8133	81.33	30.71	1.64
9		Red	0.00025	0.00004	0.00013	- 0.888	88.8	30.71	1.89
10		Blue	0.00093	0	0.0004	- 0.6453	64.53	30.4	1.122
11	Case 2 (b) current work	Green	0.0008	0	0.0003	- 0.7066	70.66	30.4	1.32
12		Red	0.00063	0	0.00024	- 0.7680	76.80	30.4	1.52
13		Blue	0.001	0.00038	0.0005	- 0.4986	49.86	30.71	0.61
14	Case 2 (c) [66]	Green	0.00068	0.00038	0.00025	- 0.6506	65.06	30.71	1.11
15		Red	0.00017	0.00035	0.00005	- 0.848	84.80	30.71	1.76
16		Blue	0.00128	0	0.00076	- 0.4560	45.60	30.4	0.5
17	Case 2 (c) current work	Green	0.0008	0	0.00038	- 0.6853	68.53	30.4	1.25
18		Red	0.00025	0.00002	0.00005	- 0.9146	91.46	30.4	2.008
19		Blue	0.00048	0.0001	0.00052	- 0.7066	70.66	27.8	1.54
20	Case 3 (a) current work	Green	0.00115	0	0.0002	- 0.6400	64.0	29.5	1.16
21		Red	0.00093	0	0.00038	- 0.6506	65.06	30.4	1.14
22		Blue	0.00081	0	0.00038	- 0.6826	68.26	30.4	1.24
23	Case 3 (b) current work	Green	0.00097	0	0.00039	- 0.6373	63.73	30.4	1.09
24		Red	0.00093	0	0.00038	- 0.6506	65.06	30.4	1.24
25		Blue	0.0011	0.00005	0.00028	- 0.6186	61.86	31.4	0.9702
26	Case 3 (c) current work	Green	0.0002	0.00035	0.00058	- 0.6986	69.86	26	1.68
27		Red	0.00093	0	0.00038	- 0.6506	65.06	30.4	1.14
28		Blue	0.0008	0.0001	0.0003	- 0.6800	68.00	32.3	1.105
26	Case 3 (d) current work	Green	0.00073	0	0.00038	- 0.7040	70.40	30.4	1.31
30		Red	0.00093	0	0.00038	- 0.6506	65.06	30.4	1.14
31		Blue	0.00008	0.00001	0.000115	- 0.9453	94.53	15.4	5.138
32	Case 1 (a) opt. current work	Green	0.000058	0.00001	0.000104	- 0.9541	95.41	14	5.81
33		Red	0.000068	0.000015	0.000096	- 0.9522	95.22	14.3	5.65
34		Blue	0.000064	0.00001	0.00012	- 0.9482	94.82	14.3	5.63
35	Case 1 (c) opt. current work	Green	0.000058	0.00001	0.000104	- 0.9541	95.41	14	5.81
36		Red	0.00006	0.000015	0.000098	- 0.9538	95.38	14.3	5.67
37		Blue	0.000038	0.000015	0.00013	- 0.9512	95.12	14.3	5.65
38	Case 2 (a) opt. current work	Green	0.000058	0.00001	0.000104	- 0.9541	95.41	14	5.81
39		Red	0.00013	0.00001	0.000088	- 0.9392	93.92	16	4.87
40		Blue	0.00006	0.00001	0.00012	- 0.9493	94.93	14.3	5.63
41	Case 2 (b) opt. current work	Green	0.000058	0.00001	0.000104	- 0.9541	95.41	14	5.81
42		Red	0.000061	0.00001	0.000089	- 0.9573	95.73	15	5.38
43		Blue	0.00009	0.000005	0.000156	- 0.9330	93.30	14.3	5.52
44	Case 3 (a) opt. current work	Green	0.000058	0.00001	0.000104	- 0.9541	95.41	14	5.81
45		Red	0.00005	0.000015	0.00008	- 0.9613	96.31	14.3	5.72
46		Blue	0.000065	0.00001	0.00012	- 0.9480	94.80	14.3	5.62
47	Case 3 (b) opt. current work	Green	0.000058	0.00001	0.000104	- 0.9541	95.41	14	5.81
48		Red	0.000066	0.00001	0.000034	- 0.9706	97.06	13.5	6.19

Figure 10 exhibits that the displacement time response of the main mass is smaller among the secondary masses. The addition of the dynamic vibration absorber reduces system response by about 217% when compared to the system without it, as manifested in Table III. The optimization procedure is run for several combinations of system parameters (mass, springs, and damping) and the results are illustrated in Table IV. The objective is then obtained to achieve the smallest value of the time response of the main mass (M_1). It is noted that the smallest time response is attained at the second row (yellow) of 1.9522E-6 m. Table IV also shows that M_2 and ξ_2 are the parameters that demonstrate the greatest effect on the objective values. For further insight into how the time response of the main system varies with variations of the design parameters, sensitivity analysis is implemented for limited cases in the next section.
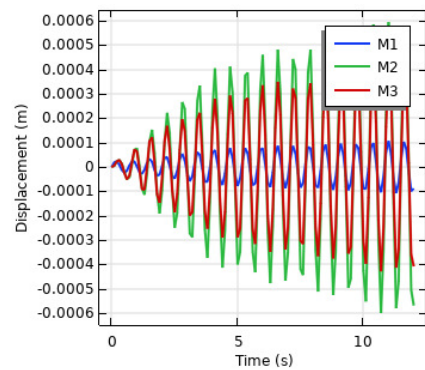
Fig. 10.   Time response of the main system at the optimal values of system parameters.

TABLE III.   OPTIMIZATION FREQUENCY RESPONSE

M_1 (kg)	M_2 (kg)	M_3 (kg)	K_1 (N/m)	K_2 (N/m)	K_3 (N/m)	ξ_1	ξ_2	ξ_3	Objective
0.01000	0.0020000	2.0000E-4	39.438	7.8870	0.78800	0.010000	0.010000	0.010000	0.0030186
0.01000	0.0020000	2.0000E-4	39.438	7.8870	0.78800	0.010000	0.010000	0.010000	0.0030186
0.01000	0.20000	2.0000E-4	39.438	7.8870	0.78800	0.010000	0.010000	0.010000	0.0029405
0.01000	0.0020000	0.10000	39.438	7.8870	0.78800	0.010000	0.010000	0.010000	0.0029167
0.01000	0.0020000	2.0000E-4	39.738	7.8870	0.78800	0.010000	0.010000	0.010000	0.0029751
.010000	0.0020000	2.0000E-4	39.438	8.1870	0.78800	0.010000	0.010000	0.010000	0.0028797
0.01000	0.0020000	2.0000E-4	39.438	7.8870	1.0880	0.010000	0.010000	0.010000	0.0029509
0.01000	0.0020000	2.0000E-4	39.438	7.8870	0.78800	0.10000	0.010000	0.010000	0.0028049
0.01000	0.0020000	2.0000E-4	39.438	7.8870	0.78800	0.010000	0.10000	0.010000	0.0028888
0.01000	0.0020000	2.0000E-4	39.438	7.8870	0.78800	0.010000	0.010000	0.20000	0.0029349
0.01000	0.046000	0.022378	39.505	7.9537	0.85467	0.030000	0.030000	0.052222	0.0027865
0.01000	0.068000	0.033467	39.538	7.9870	0.88800	0.040000	0.040000	0.073333	0.0027116

TABLE IV.   OPTIMIZATION TIME RESPONSE

M_2 (kg)	M_3 (kg)	K_2 (N/m)	K_3 (N/m)	ξ_2	ξ_3	Objective
0.0020000	2.0000E-4	7.8870	0.78800	0.010000	0.010000	1.5051E-5
0.080000	2.0000E-4	7.8870	0.78800	0.010000	0.010000	1.9522E-6
0.0020000	0.050000	7.8870	0.78800	0.010000	0.010000	1.4733E-5
0.0020000	2.0000E-4	7.5870	0.78800	0.010000	0.010000	1.5143E-5
0.0020000	2.0000E-4	7.8870	1.0880	0.010000	0.010000	1.5173E-5
0.0020000	2.0000E-4	7.8870	0.78800	0.060000	0.010000	1.5160E-5
0.0020000	2.0000E-4	7.8870	0.78800	0.010000	0.31000	1.5120E-5
0.027480	0.016468	7.7890	0.50000	0.026333	0.10800	1.6128E-5
0.041000	0.025100	7.8870	0.78800	0.010000	0.010000	1.9615E-5
0.041000	2.0000E-4	7.8870	0.78800	0.010000	0.010000	1.9660E-5
0.041000	2.0000E-4	7.8870	0.78800	0.010000	0.16000	2.0929E-5
0.041000	2.0000E-4	7.7370	0.78800	0.010000	0.010000	2.0225E-5
0.041000	2.0000E-4	7.8870	0.78800	0.035000	0.010000	1.8148E-5
0.041000	2.0000E-4	7.8870	0.93800	0.010000	0.010000	2.0041E-5
0.044250	0.0022750	7.8745	0.80050	0.012083	0.085000	2.0867E-5
0.041000	2.0000E-4	7.8870	0.78800	0.010000	0.16000	2.0929E-5
0.041000	2.0000E-4	7.7370	0.78800	0.010000	0.010000	2.0225E-5
0.041000	2.0000E-4	7.8870	0.78800	0.035000	0.010000	1.8148E-5
0.041000	2.0000E-4	7.8870	0.93800	0.010000	0.010000	2.0041E-5
0.044250	0.0022750	7.8745	0.80050	0.012083	0.085000	2.0867E-5
0.060500	2.0000E-4	7.8870	0.78800	0.022500	0.010000	1.6648E-5
0.060500	0.012650	7.8870	0.78800	0.010000	0.010000	2.9878E-5
0.060500	2.0000E-4	7.8870	0.78800	0.010000	0.010000	3.3592E-5
0.060500	2.0000E-4	7.8870	0.86300	0.010000	0.010000	3.2944E-5
0.060500	2.0000E-4	7.8120	0.78800	0.010000	0.010000	2.6584E-5
0.060500	2.0000E-4	7.8870	0.78800	0.010000	0.085000	3.0168E-5
0.067000	0.0043500	7.8620	0.81300	0.014167	0.035000	-6.2754E-5
0.070250	0.0064250	7.8495	0.82550	0.016250	0.047500	-1.8707E-5
0.069167	0.0057333	7.8537	0.72133	0.015556	0.043333	-2.9955E-5
0.067000	0.0043500	7.8620	0.75675	0.014167	0.035000	-6.1300E-5

0.073500	0.0022750	7.8745	0.80050	0.012083	0.022500	-1.3952E-5
0.063750	0.0022750	7.8745	0.80050	0.018333	0.022500	-4.7842E-5
0.063750	0.0022750	7.8370	0.80050	0.012083	0.022500	-7.6904E-5
0.063750	0.0085000	7.8745	0.80050	0.012083	0.022500	-1.7223E-5
0.063750	0.0022750	7.8745	0.80050	0.012083	0.060000	-5.7147E-5
0.063750	0.0022750	7.8745	0.83800	0.012083	0.022500	-6.1861E-5
0.055083	0.0050417	7.8578	0.81717	0.014861	0.039167	2.4138E-5
0.068896	0.0029667	7.8703	0.80467	0.012778	0.026667	-3.3283E-5
0.065375	0.0033125	7.8495	0.80675	0.013125	0.028750	-8.0711E-5
0.063750	0.0022750	7.8558	0.81925	0.012083	0.022500	-7.3608E-5
0.063750	0.0022750	7.8558	0.80050	0.012083	0.041250	-6.1890E-5
0.063750	0.0022750	7.8558	0.80050	0.015208	0.022500	-5.6898E-5
0.063750	0.0053875	7.8558	0.80050	0.012083	0.022500	-6.8551E-5
0.068625	0.0022750	7.8558	0.80050	0.012083	0.022500	-3.7867E-5
0.059417	0.0036583	7.8474	0.80883	0.013472	0.030833	2.4522E-5
0.066323	0.0026208	7.8537	0.80258	0.012431	0.024583	-8.0569E-5
0.075875	0.0033125	7.8495	0.80675	0.013125	0.028750	-7.8168E-6
0.065375	0.013813	7.8495	0.80675	0.013125	0.028750	-8.3596E-5
0.065375	0.0033125	7.8390	0.80675	0.013125	0.028750	-8.1756E-5
0.065375	0.0033125	7.8495	0.81725	0.013125	0.028750	-8.0086E-5
0.065375	0.0033125	7.8495	0.80675	0.023625	0.028750	-5.5067E-5
0.065375	0.0033125	7.8495	0.80675	0.013125	0.018250	-8.0870E-5
0.054875	0.0068125	7.8460	0.81025	0.016625	0.025250	2.2975E-5
0.070625	0.0041875	7.8486	0.80763	0.014000	0.027875	-1.5098E-5
0.060125	0.0059375	7.8469	0.80938	0.015750	0.026125	5.0538E-6
0.068000	0.0046250	7.8482	0.80806	0.014437	0.027437	-4.4730E-5
0.062750	0.0055000	7.8473	0.80894	0.015313	0.026562	-4.8249E-5
0.064063	0.0052812	7.8475	0.80872	0.015094	0.026781	-6.7587E-5
0.065266	0.0043516	7.8485	0.80779	0.018539	0.027711	-7.0429E-5
0.066651	0.0051901	7.8476	0.80863	0.012961	0.026872	-6.8277E-5
0.066004	0.0052129	7.8476	0.80865	0.013494	0.026850	-7.8625E-5
0.065607	0.0059910	7.8468	0.80943	0.010000	0.026071	-8.5282E-5
0.064824	0.0058050	7.8470	0.80924	0.011714	0.026258	-8.6335E-5
0.064233	0.0061010	7.8467	0.80954	0.010824	0.025962	-8.8631E-5
0.065072	0.0086348	7.8442	0.79807	0.011316	0.023428	-5.3270E-5
0.065299	0.0046431	7.8482	0.81246	0.012673	0.027419	-8.8382E-5
0.065047	0.0090784	7.8437	0.81047	0.011166	0.022984	-6.0405E-5
0.065293	0.0047540	7.8481	0.80768	0.012635	0.027309	-8.5614E-5
0.065019	0.0095589	7.8433	0.81078	0.011002	0.036504	-7.3263E-5
0.065286	0.0048741	7.8479	0.80776	0.012594	0.022813	-8.7978E-5
0.056809	0.0061010	7.8467	0.80954	0.010824	0.025962	2.3702E-5
0.064233	0.013526	7.8467	0.80954	0.010824	0.025962	-6.2131E-5
0.064233	0.0061010	7.8541	0.80954	0.010824	0.025962	-8.1123E-5
0.064233	0.0061010	7.8467	0.81696	0.010824	0.025962	-8.3039E-5
0.064233	0.0061010	7.8467	0.80954	0.018249	0.025962	-6.7525E-5
0.064233	0.0061010	7.8467	0.80954	0.010824	0.018537	-8.4639E-5
0.071658	0.0085759	7.8492	0.81201	0.013299	0.023487	-2.3074E-5
0.067946	0.0079571	7.8486	0.81139	0.012680	0.024105	-2.3806E-5
0.060521	0.0067197	7.8473	0.81016	0.011443	0.025343	-1.9715E-5
0.066090	0.0076478	7.8483	0.81109	0.012371	0.024415	-4.8701E-5
0.062377	0.0070291	7.8476	0.81047	0.011752	0.025033	-8.1123E-5
0.063662	1.0000E-4	7.8493	0.81211	0.013395	0.023391	-5.9466E-5
0.064233	0.0061010	7.8467	0.80954	0.010824	0.022249	-8.6060E-5
0.064233	0.0061010	7.8467	0.81325	0.010824	0.025962	-8.6909E-5
0.064233	0.0061010	7.8504	0.80954	0.010824	0.025962	-8.8946E-5
0.063305	0.0065650	7.8472	0.81000	0.011288	0.025497	-8.7982E-5
0.064233	0.0061010	7.8467	0.80954	0.014537	0.025962	-7.0422E-5
0.064233	0.0098133	7.8467	0.80954	0.010824	0.025962	-4.9688E-5
0.063924	0.0025434	7.8481	0.81093	0.012216	0.024569	-7.7580E-5
0.064233	0.0061010	7.8504	0.80954	0.010824	0.025962	-8.8946E-5

5) Sensitivity Analysis for Response Time

a) The Influence of M_2 and M_3 on Response Time

Figure 11 confirms the conclusions extracted from Table IV that the main system time response is more sensitive to the variations of M_2 than those corresponding to M_3. In addition, the optimal values of the mass M_2 do not only determine the minimum time response of the main mass, but also change its behavior. The best response is noticed when M_2 is 0.08, which is the optimal value mentioned in Table IV.

(a)

(b)
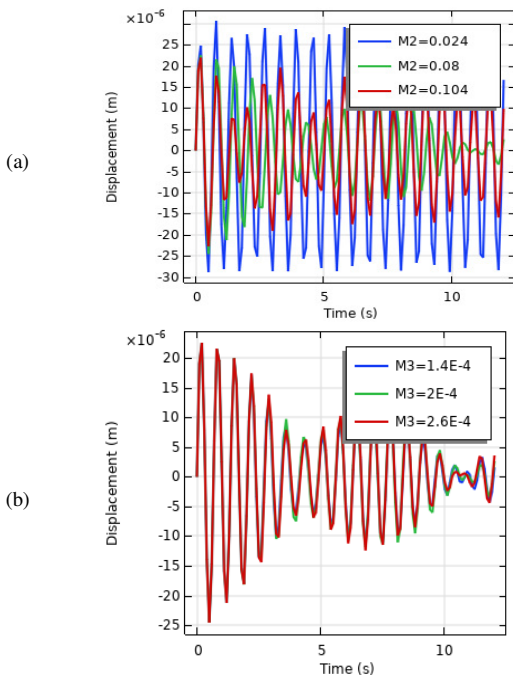
Fig. 11.   The influence of M_2 and M_3 to response time.

b)   The Influence of K_2 and K_3 on Response Time

Figure 12 depicts the nonlinear behavior of the min. mass due to the increasing values of K_2 and K_3. A similar conclusion is attained where the optimal value of K_2 (7.887 N/m) shows the smaller time response of the main mass. However, the effect of K_3 is not remarkable on the time response and no significant change in the time response is noticed.

(a)

(b)
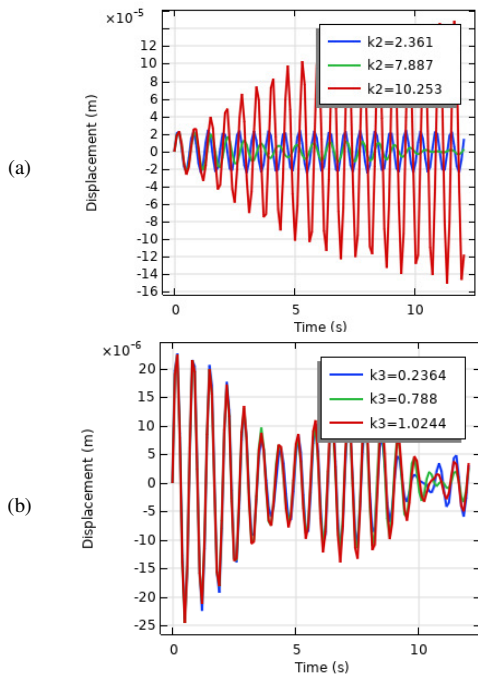
Fig. 12.   The influence of K_2 and K_3 on response time.

a)   The Influence of ξ_2 and ξ_3 on Response Time

Figure 13 illustrates the damping ratio effect on time response. The optimal value of ξ_2 shows the smaller values of the time response, while ξ_3 displays no significant changes in the time response.

(a)

(b)
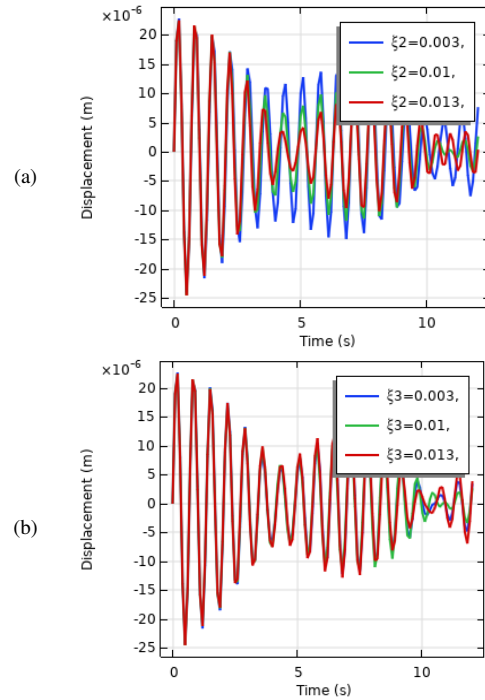
Fig. 13.   The influence of ξ_2 and ξ_3 on response time.

IV.   CONCLUSION

The effects of mass, stiffness, and damper—all of which have a significant influence on the vibration's amplitude—were investigated in this paper using finite element analysis. Several conclusions can be drawn from this work, such as:

- The results indicated that the DVA's frequency bandwidth for vibration suppression has increased.

- DVA is a useful device for achieving vibration reduction. The harmonic response frequency is shifted to the left or right of the frequency of the system when a DVA is added, depending on the DVA mass and spring values.

- Optimal performance can be achieved by selecting stiffness, damper, and mass parameters that yield the best attenuation. As a result, every DVA has fundamental values.

- It is concluded that a model with optimal parameters can widen the frequency stop-band vibration reduction and significantly lower the resonance amplitude.

- The findings demonstrated a relationship between vibration and frequency shift. When the value (Y) is greater than 1 a decrease in vibration is indicated and vice versa. The largest reduction in vibration amplitude was shown in Case-2 (red) for frequency response, with an average decrease of

91.46% and Y = 2.008 for all three modes. On the other hand, with an average decrease of 97.06% and Y = 6.19 for all three modes, optimization Case 3 (red) demonstrated the greatest value. In the second scenario, Case 2 (blue) was the worst (45.60%) with Y = 0.5. Adding more DVA units can further lower vibration amplitude, but only if they are positioned correctly.

- The DVA mass has a major impact on the system's basic frequency. Moreover, applying the proper parameters quickly dissipates the transitory vibration, reduces the base mass's vibrational amplitude, and activates the vibration absorber.

- The time response of the main mass is smaller than that of the secondary masses. The addition of the dynamic vibration absorber reduces system response greatly.

- The Nelder-Mead method improved the reduction of vibration to 97.06 %.

REFERENCES

[1] H. Frahm, "Device for damping vibrations of bodies," US989958A, Apr. 18, 1911.

[2] J. C. Snowdon and D. I. G. Jones, "Vibration and Shock in Damped Mechanical Systems," *Journal of Applied Mechanics*, vol. 36, no. 2, Jun. 1969, Art. no. 383, https://doi.org/10.1115/1.3564684.

[3] R. G. Jacquot and J. E. Foster, "Optimal Cantilever Dynamic Vibration Absorbers," *Journal of Engineering for Industry*, vol. 99, no. 1, pp. 138–141, Feb. 1977, https://doi.org/10.1115/1.3439127.

[4] R. G. Jacquot, "Optimal dynamic vibration absorbers for general beam systems," *Journal of Sound and Vibration*, vol. 60, no. 4, pp. 535–542, Oct. 1978, https://doi.org/10.1016/S0022-460X(78)80090-X.

[5] S. E. Randall, D. M. Halsted III, and D. L. Taylor, "Optimum Vibration Absorbers for Linear Damped Systems," *Journal of Mechanical Design*, vol. 103, no. 4, pp. 908–913, Oct. 1981, https://doi.org/10.1115/1.3255005.

[6] L. Zuo and S. A. Nayfeh, "Minimax optimization of multi-degree-of-freedom tuned-mass dampers," *Journal of Sound and Vibration*, vol. 272, no. 3, pp. 893–908, May 2004, https://doi.org/10.1016/S0022-460X(03)00500-5.

[7] J. Fortgang and W. Singhose, "Design of Vibration Absorbers for Step Motions and Step Disturbances," *Journal of Mechanical Design*, vol. 127, no. 1, pp. 160–163, Mar. 2005, https://doi.org/10.1115/1.1825441.

[8] K. Liu and G. Coppola, "Optimal design of damped dynamic vibration absorber for damped primary systems," *Transactions of the Canadian Society for Mechanical Engineering*, vol. 34, no. 1, pp. 119–135, Mar. 2010, https://doi.org/10.1139/tcsme-2010-0008.

[9] K. Liu and J. Liu, "The damped dynamic vibration absorbers: revisited and new result," *Journal of Sound and Vibration*, vol. 284, no. 3, pp. 1181–1189, Jun. 2005, https://doi.org/10.1016/j.jsv.2004.08.002.

[10] L. Zuo and S. A. Nayfeh, "The Two-Degree-of-Freedom Tuned-Mass Damper for Suppression of Single-Mode Vibration Under Random and Harmonic Excitation," *Journal of Vibration and Acoustics*, vol. 128, no. 1, pp. 56–65, Apr. 2005, https://doi.org/10.1115/1.2128639.

[11] A. Ghosh and B. Basu, "A closed-form optimal tuning criterion for TMD in damped structures," *Structural Control and Health Monitoring*, vol. 14, no. 4, pp. 681–692, 2007, https://doi.org/10.1002/stc.176.

[12] W. O. Wong and Y. L. Cheung, "Optimal design of a damped dynamic vibration absorber for vibration control of structure excited by ground motion," *Engineering Structures*, vol. 30, no. 1, pp. 282–286, Jan. 2008, https://doi.org/10.1016/j.engstruct.2007.03.007.

[13] F. A. C. Viana, G. I. Kotinda, D. A. Rade, and V. Steffen, "Tuning dynamic vibration absorbers by using ant colony optimization," *Computers & Structures*, vol. 86, no. 13, pp. 1539–1549, Jul. 2008, https://doi.org/10.1016/j.compstruc.2007.05.009.

[14] R. S. Lakes, "Extreme Damping in Composite Materials with a Negative Stiffness Phase," *Physical Review Letters*, vol. 86, no. 13, pp. 2897–2900, Mar. 2001, https://doi.org/10.1103/PhysRevLett.86.2897.

[15] R. S. Lakes, "Extreme damping in compliant composites with a negative-stiffness phase," *Philosophical Magazine Letters*, vol. 81, pp. 95–100, Feb. 2001, https://doi.org/10.1080/09500830010015332.

[16] R. S. Lakes, T. Lee, A. Bersie, and Y. C. Wang, "Extreme damping in composite materials with negative-stiffness inclusions," *Nature*, vol. 410, no. 6828, pp. 565–567, Mar. 2001, https://doi.org/10.1038/35069035.

[17] R. S. Lakes and W. J. Drugan, "Dramatically stiffer elastic composite materials due to a negative stiffness phase?," *Journal of the Mechanics and Physics of Solids*, vol. 50, no. 5, pp. 979–1009, May 2002, https://doi.org/10.1016/S0022-5096(01)00116-8.

[18] Y. C. Wang and R. S. Lakes, "Extreme stiffness systems due to negative stiffness elements," *American Journal of Physics*, vol. 72, no. 1, pp. 40–50, Jan. 2004, https://doi.org/10.1119/1.1619140.

[19] Y.-C. Wang and R. Lakes, "Negative stiffness-induced extreme viscoelastic mechanical properties: stability and dynamics," *Philosophical Magazine*, vol. 84, no. 35, pp. 3785–3801, Dec. 2004, https://doi.org/10.1080/1478643042000282702.

[20] Y.-C. Wang and R. Lakes, "Stability of negative stiffness viscoelastic systems," *Quarterly of Applied Mathematics*, vol. 63, no. 1, pp. 34–55, 2005, https://doi.org/10.1090/S0033-569X-04-00938-6.

[21] J. P. Den Hartog, *Mechanical vibrations*. New York, NY, USA: McGraw Hill, 1956.

[22] J. Ormondroyd and J. P. Den Hartog, "The Theory of the Dynamic Vibration Absorber," *Transactions of the American Society of Mechanical Engineers*, vol. 49–50, no. 021007, Dec. 2023, https://doi.org/10.1115/1.4058553.

[23] T. You, J. Zhou, D. J. Thompson, D. Gong, J. Chen, and Y. Sun, "Vibration reduction of a high-speed train floor using multiple dynamic vibration absorbers," *Vehicle System Dynamics*, vol. 60, no. 9, pp. 2919–2940, Sep. 2022, https://doi.org/10.1080/00423114.2021.1928248.

[24] J. Shaw, S. W. Shaw, and A. G. Haddow, "On the response of the non-linear vibration absorber," *International Journal of Non-Linear Mechanics*, vol. 24, no. 4, pp. 281–293, Jan. 1989, https://doi.org/10.1016/0020-7462(89)90046-2.

[25] S. S. Oueini and A. H. Nayfeh, "Analysis and Application of a Nonlinear Vibration Absorber," *Journal of Vibration and Control*, vol. 6, no. 7, pp. 999–1016, Oct. 2000, https://doi.org/10.1177/107754630000600703.

[26] O. N. Ashour and A. H. Nayfeh, "Experimental and Numerical Analysis of a Nonlinear Vibration Absorber for the Control of Plate Vibrations," *Journal of Vibration and Control*, vol. 9, no. 1–2, pp. 209–234, Jan. 2003, https://doi.org/10.1177/107754603030748.

[27] R. Viguie and G. Kerschen, "Nonlinear vibration absorber coupled to a nonlinear primary system: A tuning methodology," *Journal of Sound and Vibration*, vol. 326, no. 3, pp. 780–793, Oct. 2009, https://doi.org/10.1016/j.jsv.2009.05.023.

[28] G. Habib, T. Detroux, R. Viguié, and G. Kerschen, "Nonlinear generalization of Den Hartog's equal-peak method," *Mechanical Systems and Signal Processing*, vol. 52–53, pp. 17–28, Feb. 2015, https://doi.org/10.1016/j.ymssp.2014.08.009.

[29] G. B. Warburton, "Optimum absorber parameters for minimizing vibration response," *Earthquake Engineering & Structural Dynamics*, vol. 9, no. 3, pp. 251–262, 1981, https://doi.org/10.1002/eqe.4290090306.

[30] G. B. Warburton, "Optimum absorber parameters for various combinations of response and excitation parameters," *Earthquake Engineering & Structural Dynamics*, vol. 10, no. 3, pp. 381–401, 1982, https://doi.org/10.1002/eqe.4290100304.

[31] T. Asami, O. Nishihara, and A. M. Baz, "Analytical Solutions to H∞ and H2 Optimization of Dynamic Vibration Absorbers Attached to Damped Linear Systems," *Journal of Vibration and Acoustics*, vol. 124, no. 2, pp. 284–295, Mar. 2002, https://doi.org/10.1115/1.1456458.

[32] J. P. D. Hartog, *Mechanical Vibrations*. Chelmsford, MA, USA: Courier Corporation, 1985.

[33] V. Piccirillo, A. M. Tusset, and J. M. Balthazar, "Optimization of dynamic vibration absorbers based on equal-peak theory," *Latin American Journal of Solids and Structures*, vol. 16, no. 4, Apr. 2019, Art. no. e184, https://doi.org/10.1590/1679-78255285.

[34] Y. Hao, Y. Shen, X. Li, J. Wang, and S. Yang, "H∞ optimization of Maxwell dynamic vibration absorber with multiple negative stiffness springs," *Journal of Low Frequency Noise, Vibration and Active Control*, vol. 40, no. 3, pp. 1558–1570, Sep. 2021, https://doi.org/10.1177/1461348420972818.

[35] Y. Hua, W. Wong, and L. Cheng, "Optimal design of a beam-based dynamic vibration absorber using fixed-points theory," *Journal of Sound and Vibration*, vol. 421, pp. 111–131, May 2018, https://doi.org/10.1016/j.jsv.2018.01.058.

[36] O. Nishihara, "Exact Optimization of a Three-Element Dynamic Vibration Absorber: Minimization of the Maximum Amplitude Magnification Factor," *Journal of Vibration and Acoustics*, vol. 141, no. 1, Jul. 2018, Art. no. 011001, https://doi.org/10.1115/1.4040575.

[37] Y. Shen, Z. Xing, S. Yang, and J. Sun, "Parameters optimization for a novel dynamic vibration absorber," *Mechanical Systems and Signal Processing*, vol. 133, Nov. 2019, Art. no. 106282, https://doi.org/10.1016/j.ymssp.2019.106282.

[38] E. Barredo, J. G. Mendoza Larios, J. Mayén, A. A. Flores-Hernández, J. Colín, and M. Arias Montiel, "Optimal design for high-performance passive dynamic vibration absorbers under random vibration," *Engineering Structures*, vol. 195, pp. 469–489, Sep. 2019, https://doi.org/10.1016/j.engstruct.2019.05.105.

[39] Z.-D. Xu, X.-H. Huang, F.-H. Xu, and J. Yuan, "Parameters optimization of vibration isolation and mitigation system for precision platforms using non-dominated sorting genetic algorithm," *Mechanical Systems and Signal Processing*, vol. 128, pp. 191–201, Aug. 2019, https://doi.org/10.1016/j.ymssp.2019.03.031.

[40] J. Dai, Z.-D. Xu, P.-P. Gai, and Z.-W. Hu, "Optimal design of tuned mass damper inerter with a Maxwell element for mitigating the vortex-induced vibration in bridges," *Mechanical Systems and Signal Processing*, vol. 148, Feb. 2021, Art. no. 107180, https://doi.org/10.1016/j.ymssp.2020.107180.

[41] Y. Shen, Z. Xing, S. Yang, and X. Li, "Optimization and analysis of a grounded type dynamic vibration absorber with lever component," *Science Progress*, vol. 103, no. 4, Oct. 2020, Art. no. 0036850420959889, https://doi.org/10.1177/0036850420959889.

[42] M. Liu, Y. Zhang, J. Huang, and C. Zhang, "Optimization control for dynamic vibration absorbers and active suspensions of in-wheel-motor-driven electric vehicles," *Proceedings of the Institution of Mechanical Engineers, Part D: Journal of Automobile Engineering*, vol. 234, no. 9, pp. 2377–2392, Aug. 2020, https://doi.org/10.1177/0954407020908667.

[43] O. A. Charef and S. Khalfallah, "H-infinity optimization of dynamic vibration absorber with negative stiffness," *Acta Technica Napocensis Series-Applied Mathematics Mechanics and Engineering*, vol. 64, no. 3, pp. 461–468, Oct. 2021.

[44] Y. Qin, J. J. Tan, and M. C. J. Hornikx, "Optimization of multiple dynamic vibration absorbers for reduction of low frequency vibration of joist floor structures," in *EuroNoise 2021*, Madeira, Portugal, Oct. 2021, pp. 343–354.

[45] P. V. R. Raj and B. Santhosh, "Parametric study and optimization of linear and nonlinear vibration absorbers combined with piezoelectric energy harvester," *International Journal of Mechanical Sciences*, vol. 152, pp. 268–279, Mar. 2019, https://doi.org/10.1016/j.ijmecsci.2018.12.053.

[46] X. Wang, X. Liu, Y. Shan, Y. Shen, and T. He, "Analysis and Optimization of the Novel Inerter-Based Dynamic Vibration Absorbers," *IEEE Access*, vol. 6, pp. 33169–33182, Jan. 2018, https://doi.org/10.1109/ACCESS.2018.2844086.

[47] X. Wang, T. He, Y. Shen, Y. Shan, and X. Liu, "Parameters optimization and performance evaluation for the novel inerter-based dynamic vibration absorbers with negative stiffness," *Journal of Sound and Vibration*, vol. 463, Dec. 2019, Art. no. 114941, https://doi.org/10.1016/j.jsv.2019.114941.

[48] W. R. Johnson and M. Ruzzene, "Challenges and constraints in the application of resonance-based metamaterials for vibration isolation," in

[49] D. L. Platus, "Negative-stiffness-mechanism vibration isolation systems," in *Vibration Control in Microelectronics, Optics, and Metrology*, San Jose, CA, USA, Nov. 1991, vol. 1619, pp. 44–54, https://doi.org/10.1117/12.56823.

[50] T. Mizuno, T. Toumiya, and M. Takasaki, "Vibration Isolation System Using Negative Stiffness," *JSME International Journal Series C Mechanical Systems, Machine Elements and Manufacturing*, vol. 46, no. 3, pp. 807–812, 2003, https://doi.org/10.1299/jsmec.46.807.

[51] H. Xiuchang, S. Zhiwei, and H. Hongxing, "Optimal parameters for dynamic vibration absorber with negative stiffness in controlling force transmission to a rigid foundation," *International Journal of Mechanical Sciences*, vol. 152, pp. 88–98, Mar. 2019, https://doi.org/10.1016/j.ijmecsci.2018.12.033.

[52] M. A. Acar and C. Yilmaz, "Design of an adaptive–passive dynamic vibration absorber composed of a string–mass system equipped with negative stiffness tension adjusting mechanism," *Journal of Sound and Vibration*, vol. 332, no. 2, pp. 231–245, Jan. 2013, https://doi.org/10.1016/j.jsv.2012.09.007.

[53] J. Yang, Y. P. Xiong, and J. T. Xing, "Dynamics and power flow behaviour of a nonlinear vibration isolation system with a negative stiffness mechanism," *Journal of Sound and Vibration*, vol. 332, no. 1, pp. 167–183, Jan. 2013, https://doi.org/10.1016/j.jsv.2012.08.010.

[54] R. Zivieri, "Dynamical Properties of a Periodic Mass-Spring Nonlinear Seismic Metamaterial," in *Fourteenth International Congress on Artificial Materials for Novel Wave Phenomena (Metamaterials)*, New York, NY, USA, Oct. 2020, pp. 12–14, https://doi.org/10.1109/Metamaterials49557.2020.9285057.

[55] Y. Wang, H.-X. Li, C. Cheng, H. Ding, and L.-Q. Chen, "A nonlinear stiffness and nonlinear inertial vibration isolator," *Journal of Vibration and Control*, vol. 27, no. 11–12, pp. 1336–1352, Jun. 2021, https://doi.org/10.1177/1077546320940924.

[56] J. P. D. Hartog, *Mechanical Vibrations*. New York, NY, USA: Dover Publications, 1981.

[57] D. T. Hang, N. X. Tung, D. V. Tu, and N. N. Lam, "Finite Element Analysis of a Double Beam connected with Elastic Springs," *Engineering, Technology & Applied Science Research*, vol. 14, no. 1, pp. 12482–12487, Feb. 2024, https://doi.org/10.48084/etasr.6489.

[58] R. O. Duda, P. E. Hart, P. E. Hart, and D. G. Stork, *Pattern Classification*. Hoboken, NJ, USA: Wiley, 2000.

[59] K. I. M. McKinnon, "Convergence of the Nelder--Mead Simplex Method to a Nonstationary Point," *SIAM Journal on Optimization*, vol. 9, no. 1, pp. 148–158, Jan. 1998, https://doi.org/10.1137/S1052623496303482.

[60] T. G. Kolda, R. M. Lewis, and V. Torczon, "Optimization by Direct Search: New Perspectives on Some Classical and Modern Methods," *SIAM Review*, vol. 45, no. 3, pp. 385–482, Jan. 2003, https://doi.org/10.1137/S003614450242889.

[61] J. A. Nelder and R. Mead, "A Simplex Method for Function Minimization," *The Computer Journal*, vol. 7, no. 4, pp. 308–313, Jan. 1965, https://doi.org/10.1093/comjnl/7.4.308.

[62] W. Spendley, G. R. Hext, and F. R. Himsworth, "Sequential Application of Simplex Designs in Optimisation and Evolutionary Operation," *Technometrics*, vol. 4, no. 4, pp. 441–461, Nov. 1962, https://doi.org/10.1080/00401706.1962.10490033.

[63] P. F. Pai, "Metamaterial-based Broadband Elastic Wave Absorber," *Journal of Intelligent Material Systems and Structures*, vol. 21, no. 5, pp. 517–528, Mar. 2010, https://doi.org/10.1177/1045389X09359436.

[64] H. Peng, P. Frank Pai, and H. Deng, "Acoustic multi-stopband metamaterial plates design for broadband elastic wave absorption and vibration suppression," *International Journal of Mechanical Sciences*, vol. 103, pp. 104–114, Nov. 2015, https://doi.org/10.1016/j.ijmecsci.2015.08.024.

[65] P. F. Pai and M. J. Sundaresan, "Actual working mechanisms of smart metamaterial structures," in *Health Monitoring of Structural and Biological Systems*, San Diego, CA, USA, Mar. 2013, vol. 8695, pp. 725–741, https://doi.org/10.1117/12.2009792.

Health Monitoring of Structural and Biological Systems XII, Mar. 2018, vol. 10600, pp. 489–500, https://doi.org/10.1117/12.2294919.

[66] H. Deng, "Elastic Wave Absorption in Laser-Cut Acoustic Metamaterial Plates," Ph.D. dissertation, University of Missouri, Columbia, MO, USA, 2016.

[67] S. Jiang, "Finite-element design of metamaterial beams for broadband wave absorption," M.S. thesis, University of Missouri, Columbia, MO, USA, 2015.

[68] F. A. Jabbar and P. S. Rao, "Vibration attenuation and frequency shifting of beam structures using single and multiple dynamic absorbers in the parallel," *Archive of Mechanical Engineering*, vol. 70, no. 4, pp. 457–480, 2023.